

 Open access • Journal Article • DOI:10.1029/2006JD007971

Nitrogen oxide measurements at rural sites in Switzerland : Bias of conventional measurement techniques — [Source link](#)

Martin Steinbacher, Christoph Zellweger, Beat Schwarzenbach, S. Bugmann ...+4 more authors





Institutions: Swiss Federal Laboratories for Materials Science and Technology, Paul Scherrer Institute

Published on: 16 Jun 2007 - Journal of Geophysical Research (John Wiley & Sons, Ltd)

Topics: Ultraviolet light

Related papers:

- [Evaluation of nitrogen dioxide chemiluminescence monitors in a polluted urban environment](#)
- [Response of commercial chemiluminescent nitric oxide-nitrogen dioxide analyzers to other nitrogen-containing compounds](#)
- [Ground-level nitrogen dioxide concentrations inferred from the satellite-borne Ozone Monitoring Instrument](#)
- [Atmospheric Chemistry and Physics: From Air Pollution to Climate Change](#)
- [Validation of urban NO₂ concentrations and their diurnal and seasonal variations observed from the SCIAMACHY and OMI sensors using in situ surface measurements in Israeli cities](#)

Share this paper:    

View more about this paper here: <https://typeset.io/papers/nitrogen-oxide-measurements-at-rural-sites-in-switzerland-4xmv1lisxj>



Nitrogen oxide measurements at rural sites in Switzerland: Bias of conventional measurement techniques

M. Steinbacher,¹ C. Zellweger,¹ B. Schwarzenbach,¹ S. Bugmann,¹ B. Buchmann,¹
C. Ordóñez,^{2,3} A. S. H. Prevot,² and C. Hueglin¹

Received 28 August 2006; revised 30 January 2007; accepted 2 March 2007; published 12 June 2007.

[1] Nitrogen oxides ($\text{NO}_x = \text{NO} + \text{NO}_2$) in the atmosphere are often measured using instruments equipped with molybdenum converters. NO_2 is catalytically converted to NO on a heated molybdenum surface and subsequently measured by chemiluminescence after reaction with ozone. The drawback of this technique is that other oxidized nitrogen compounds such as peroxyacetyl nitrate and nitric acid are also partly converted to NO. Thus such NO_2 measurements are really surrogate NO_2 measurements because the resultant values systematically overestimate the true value because of interferences of these compounds, especially when sampling photochemically aged air masses. However, molybdenum converters are widely used, and a dense network of surrogate NO_2 measurements exists. As an alternative with far less interference, photolytic converters using ultraviolet light are nowadays applicable also for long-term measurements. This work presents long-term collocated NO_2 measurements using molybdenum and photolytic converters at two rural sites in Switzerland. On a relative scale, the molybdenum converter instruments overestimate the NO_2 concentrations most during spring/summer because of prevalent photochemistry. On a monthly basis, only 70–83% of the “surrogate” NO_2 can be attributed to “real” NO_2 at the non-elevated site and even less (43–76%) at the elevated one. The observed interferences have to be taken into account for monitoring and regulatory issues and to be considered when using these data for ground-truthing of satellite data or for validation of chemical transport models. Alternatively, an increased availability of artifact-free data would also be beneficial for these issues.

Citation: Steinbacher, M., C. Zellweger, B. Schwarzenbach, S. Bugmann, B. Buchmann, C. Ordóñez, A. S. H. Prevot, and C. Hueglin (2007), Nitrogen oxide measurements at rural sites in Switzerland: Bias of conventional measurement techniques, *J. Geophys. Res.*, 112, D11307, doi:10.1029/2006JD007971.

1. Introduction

[2] Nitrogen oxides ($\text{NO}_x = \text{NO} + \text{NO}_2$) originating from combustion, lightning, and soils largely control tropospheric ozone production [Hauglustaine *et al.*, 2001; Henne *et al.*, 2005; Jacob *et al.*, 1996; Penner *et al.*, 1991]. However, considerable uncertainty exists in the magnitude and distribution of NO_x emissions [Emmons *et al.*, 1997; Lee *et al.*, 1997]. Global mapping of atmospheric nitrogen dioxide (NO_2) concentrations from space provides critical information for constraining NO_x emissions [e.g., Jaegle *et al.*, 2005; Martin *et al.*, 2006; Richter *et al.*, 2005] and more generally improves our understanding of tropospheric chemistry. On the other hand, in situ observations offer

the possibility to gather information on the regional NO_x distribution with high time resolution.

[3] Currently, most commercially available NO_2 instruments for ground-based measurements use molybdenum converters heated to 300°–400°C. With presence of oxygen, NO_2 is reduced to nitrogen monoxide (NO) whereas the Mo surface is oxidized to MoO_2 and MoO_3 . The subsequent analysis of NO is done by chemiluminescence after reaction with ozone. Already, decades ago, several laboratory studies showed that the conversion is not specific to NO_2 . Oxidized nitrogen compounds such as nitric acid (HNO_3), peroxyacetyl nitrate (PAN), and other organic nitrates may also be reduced to NO [Gehrig and Baumann, 1993; Grosjean and Harrison, 1985; Winer *et al.*, 1974]. In consequence, these compounds can significantly interfere with the measurements by contributing to the NO_2 signal and thus leading to an overestimated NO_2 measurement under certain conditions. Therefore NO_x data obtained with molybdenum converters have to be considered with caution. NO_2 measurements with this converter type show reasonable results in urban areas when the total odd nitrogen ($\equiv \text{NO}_y = \text{NO}_x + \text{HNO}_3 + \text{PAN} + \text{HONO} + \text{HO}_2\text{NO}_2 + \text{NO}_3 + \text{N}_2\text{O}_5 + \text{other organic nitrogen-containing com-}$

¹Laboratory for Air Pollution/Environmental Technology, Empa, Swiss Federal Laboratories for Materials Testing and Research, Dübendorf, Switzerland.

²Laboratory of Atmospheric Chemistry, Paul Scherrer Institute, Villigen PSI, Switzerland.

³Laboratoire d'Aérodologie, Toulouse, France.

pounds) concentration is usually dominated by NO_x , and thus interferences of HNO_3 and PAN and also of the other species are relatively small. In rural and remote locations as well as in substantially aged air masses where NO_x is small compared with NO_y , the measurements are not well defined and lead to overestimated results.

[4] Already in the 1970s, laboratory experiments showed that PAN, ethyl nitrate, and ethyl nitrite were converted to NO with an efficiency of 92, 103, and 92%, respectively [Winer *et al.*, 1974]. A response of HNO_3 was also detected but could not be quantified. Measurements performed by Grosjean and Harrison [1985] revealed conversion efficiencies of the molybdenum converter at 450°C for nitric acid, PAN, methyl nitrate, *n*-propyl nitrate, and *n*-butyl nitrate of more than 98%. Dunlea *et al.* [2007] performed comparisons of NO_2 measured with molybdenum converters and tunable diode laser absorption spectroscopy (TDLAS) and differential absorption spectroscopy (DOAS) in Mexico City and attributed the enhanced NO_2 concentrations measured with molybdenum converters mainly to HNO_3 and alkyl and multifunctional alkyl nitrates. Since HNO_3 is known for (temperature- and humidity-dependent) losses and memory effects in the inlet system [Neuman *et al.*, 1999; Volz-Thomas *et al.*, 2005], these interferences can depend on the specific design and implementation of the inlet and thus may be less pronounced but still of considerable importance for field measurements. Memory effects are mainly a problem for conditions with strongly varying atmospheric concentrations.

[5] Fehsenfeld *et al.* [1987, 1988] intercompared surface converter/chemiluminescence detectors with photolytic converters during field campaigns in Colorado in the 1980s [Fehsenfeld *et al.*, 1987, 1988]. They used hydrated, crystalline ferrous sulphate (FeSO_4) instead of molybdenum for the surface reduction of NO_2 to NO and reported significant interferences of *n*-propyl nitrate and PAN as well as considerable memory effects and humidity dependencies. As a consequence, they did not recommend FeSO_4 converters for measuring NO_2 . Fehsenfeld *et al.* [1987] employed a molybdenum converter heated to 400°C to measure NO_y , which was intercompared with a gold converter and 0.3% of CO as the reducing agent. The results confirmed that NO_y rather than NO_x was detected with this setup. Williams *et al.* [1998] compared different molybdenum converters (340°–375°C, at ambient pressure) used for NO_y measurements with two gold converters and found only small differences in the NO_y concentration. Spiking tests with HNO_3 did not reveal satisfying recoveries for all converters. Commercial NO_2 instruments using a molybdenum converter are usually operated under low-pressure conditions at temperatures between 300° and 350°C. In contrast to molybdenum converters, no interferences or artifacts were reported for the photolysis of NO_2 by ultraviolet light by Fehsenfeld *et al.* [1990]. However, Ryerson *et al.* [2000] did an extensive assessment of potential interferences for photolytic converters and estimated a HONO conversion efficiency of 37%. The manufacturer (Ecophysics) of the photolytic converter used in the present study specifies a HONO interference of lower than 20%. Negative interferences were reported for a photolytic converter employed under polluted conditions in a road tunnel because of chemical reactions with hydro-

carbons in the photolytic converter [Kurtenbach *et al.*, 2001].

[6] Besides chemiluminescence detectors coupled with NO_2 converters, there are also other techniques available to measure NO_2 at atmospheric levels, for example, DOAS [Alicke *et al.*, 2002; Platt and Perner, 1980], detection by chemiluminescence produced during the reaction with luminol [Kelly *et al.*, 1990], TDLAS [Li *et al.*, 2004], laser-induced fluorescence (LIF) [Cleary *et al.*, 2002; Day *et al.*, 2002; Thornton *et al.*, 2000], or cavity ring-down spectroscopy [Kebabian *et al.*, 2005; Osthoff *et al.*, 2006].

[7] Comparisons of photolytic converter-chemiluminescence detectors with other techniques were recently published, for example, by Thornton *et al.* [2003], who compared a photolytic converter instrument with LIF and DOAS. The photolysis/chemiluminescence and the LIF instruments showed an agreement (with an average difference of less than 5%) within the combined uncertainties for the accuracy of the instruments. A good agreement was also observed with results from the DOAS system for a 2-day period. Nakamura *et al.* [2003] compared a photolytic converter instrument with two LIF instruments. Their laboratory tests revealed agreements with the LIF instruments of less than 10% difference. A high correlation was also reported by Osthoff *et al.* [2006], who compared a photolysis/chemiluminescence instrument with cavity ring-down spectroscopy. In conclusion, these various inter-comparisons among different measurement techniques indicate the absence of considerable atmospheric interferences and support our approach to use the photolysis/chemiluminescence instrument as an appropriate reference.

[8] Gerboles *et al.* [2003] assessed the uncertainty of the NO_2 measurements using molybdenum converter/chemiluminescence reaction and showed that the molybdenum converter efficiency is not affected by humidity. However, they reported that significant quenching (up to 8%) can occur in the chemiluminescence detector when the water content is increased from dry air to 80% relative humidity. Hayden *et al.* [2003] reported similar humidity dependence for a chemiluminescence NO analyzer from Ecophysics (CLD770). Our tests revealed similar quenching effects of about 2.5% (Horiba), 7% (Monitor Labs), 8% [Thermo Environmental Instruments (TEI)], and 7% (Ecophysics). Horiba instruments exhibit reduced humidity dependence due to an integrated heated permeation capillary drier. The quenching rate constant of excited NO_2 with water was investigated to be up to six times faster than with N_2 and O_2 [Donnelly *et al.*, 1979].

[9] Despite all drawbacks of this conversion technique, molybdenum converters are still widely used and are the most common technique for long-term “surrogate” NO_2 monitoring. Therefore photolysis converters were so far mainly operated during temporally limited field campaigns [Acker *et al.*, 2005; Fahey *et al.*, 1986; Fehsenfeld *et al.*, 1987, 1990; Thornberry *et al.*, 2001] or aircraft studies [Brunner *et al.*, 2001]. Data sets using photolysis converters are rarely extended to longer periods [Hayden *et al.*, 2003; Mannošchreck *et al.*, 2004; Munger *et al.*, 1996; Zellweger *et al.*, 2003].

[10] The main objective of this study is the analysis of two long-term NO_2 measurement time series using different techniques at two rural sites at different altitudes in

Switzerland. The results allow estimating the diurnal and seasonal as well as the meteorological influence of interfering compounds on surrogate NO₂ measurements performed with commercial molybdenum converter monitors. The consideration of these interferences should not be ignored for model-measurement intercomparisons. Moreover, these interferences were recently considered when surrogate NO₂ data were used for ground-truthing of satellite data by *Ordóñez et al.* [2006] and *Schaub et al.* [2006].

2. Experimental

2.1. Measurement Sites

[11] This study was carried out at three rural sites of the Swiss National Air Pollution Monitoring Network (NABEL):

[12] “Taenikon” [47°28′N, 8°54′E, 539 m above sea level (asl)] is a measurement site in the eastern part of the Swiss Plateau north of the Alps. The surroundings of the site are rural with moderate population. The station is slightly influenced by local traffic and a nearby (3 km NE) highway. The largest town close to the station is Winterthur (population 100,000; 12 km WNW). Several smaller villages with a few hundreds to thousands inhabitants are also in the vicinity. The annual mean temperature is 8.8°C. Monthly mean temperatures range from −0.4°C in January to 17.5°C in July.

[13] “Rigi-Seebodenalp” (47°04′N, 8°27′E, 1031 m asl) is situated in an elevated rural environment 600 m above Lake Lucerne. The station is located approximately 300 m southwest of the upper station of the cable car to Seebodenalp. The environment is rural with patches of wood and grasslands in the vicinity. Nearby cities are Lucerne (population approximately 60,000) and Zug (population approximately 20,000), both located at 12 km distance at 600 m lower altitude. Because of the elevation, the station is often influenced by relatively unpolluted air masses. Similar transport processes as described by *Zellweger et al.* [2003] and *Steinbacher et al.* [2004] are likely to influence the site. In addition, the sampling site is located close to a northwest exposed slope that often induces a southeasterly downslope wind between sunset and sunrise [*Steinbacher et al.*, 2004]. The annual mean temperature is 7.2°C. Monthly mean temperatures range from −1.0°C in February to 16.1°C in July.

[14] For validation of the calculated correction factors, the results obtained at Taenikon were applied to data observed at “Payerne” (46°49′N, 6°57′E, 489 m asl), a measurement site in the western part of the Swiss Plateau located in a rural environment approximately 1 km SE of Payerne, a village with 8000 inhabitants. The situation in terms of air pollution and meteorological conditions is similar to the conditions at Taenikon.

[15] All stations are jointly operated by Empa and the Swiss Federal Office for the Environment (FOEN) and are also part of the EMEP program (Cooperative Program for Monitoring and Evaluation of the Long-range Transmission of Air Pollution in Europe). The stations are air-conditioned to 22°C, and the standardized NABEL inlet configuration is in use at both stations. It consists of an inlet tube made out of Ematal-coated aluminum outside the station [inner dia-

meter (ID) 4 cm, length 1 to 1.5 m] and a glass manifold (ID 4 cm, inside the station), both flushed with 250 l/min. Perfluoroalkoxy (PFA) Teflon tubes [outer diameter (OD) 6 mm, approximately 2 m] are used in the stream to connect the instruments to the glass inlet. The residence times in the inlet system are approximately 0.5, 0.9, and 3.5 sec for the aluminum, the glass, and the PFA parts of the inlet, respectively. Because of the short residence times, the formation of NO₂ via the reaction of O₃ with NO in the inlet system is negligible.

2.2. Instrumental

[16] NO₂ measurements with a photolytic converter were made with a Cranox instrument (Ecophysics, Duernten, Switzerland) using a chemiluminescence detector (CLD 770 AL) for the detection of NO. NO₂ was photolytically converted to NO (PLC 760) before detection. An automatic calibration of the instrument was performed every 23 h. The chemiluminescence detector was calibrated with NO standard gas (5 ± 0.1 ppmv NO in N₂, diluted with zero air to 30 ppbv) and zero air (dew point −20°C). The conversion efficiency of the converter was determined by gas phase titration of NO with ozone. The conversion efficiency of the PLC ranged from 30 to 65%. The NO standard mixture (NO 99.8% in N₂ 99.999%, Messer-Griesheim GmbH) was traced back to the National Institute of Standards and Technology (NIST) Reference Material. Overall uncertainties for 1-h averages are estimated to be ±5% for NO and ±10% for NO₂ at ambient levels of 500 ppt (1σ) [*Zellweger et al.*, 2000]. They include the precision of the CLD, the NO standard uncertainty, and the conversion efficiencies of the PLC.

[17] NO₂ measurements with molybdenum converters were made using instruments from Horiba, Monitor Labs, and TEI. The same standards were used as for the photolytic converter system. The molybdenum converter temperature ranged from 300°–320°C. Converter efficiencies were determined once a year and were always >98%. Measurement uncertainties for 1-h averages ranged from 4.3 to 6.7% (NO) and from 6.1 to 9.4% (NO₂) [*NABEL*, 2005], depending on the instrument. At low mixing ratios, minimum absolute uncertainties for both NO and NO₂ ranged from 0.2 to 2.0 ppb depending on the instrument. Interferences of other compounds to the conversion to NO were not considered.

[18] PAN measurements were performed with gas chromatography (HP 5890A; column 10% Carbowax 600 on Supelcoport 80–100 mesh) and an electron capture detector (ECD). Calibration was done with a solution containing PAN that was injected into a separation column to isolate PAN from the by-products. For further details, see *Wunderli and Gehrige* [1991].

[19] Daily samples of total nitrate, i.e., the sum of particulate nitrate (p-NO₃[−]) and gaseous nitric acid (HNO₃), were analyzed off-line after collection on alkaline-impregnated filters (Whatman-Schleicher & Schuell, Switzerland) and are presented here in HNO₃ equivalents.

[20] Additionally, data of other atmospheric species continuously measured within the NABEL network including O₃ (UV absorption), CO (nondispersive infrared detection), SO₂ (UV fluorescence), and total suspended particles (daily values collected with high volume samplers).

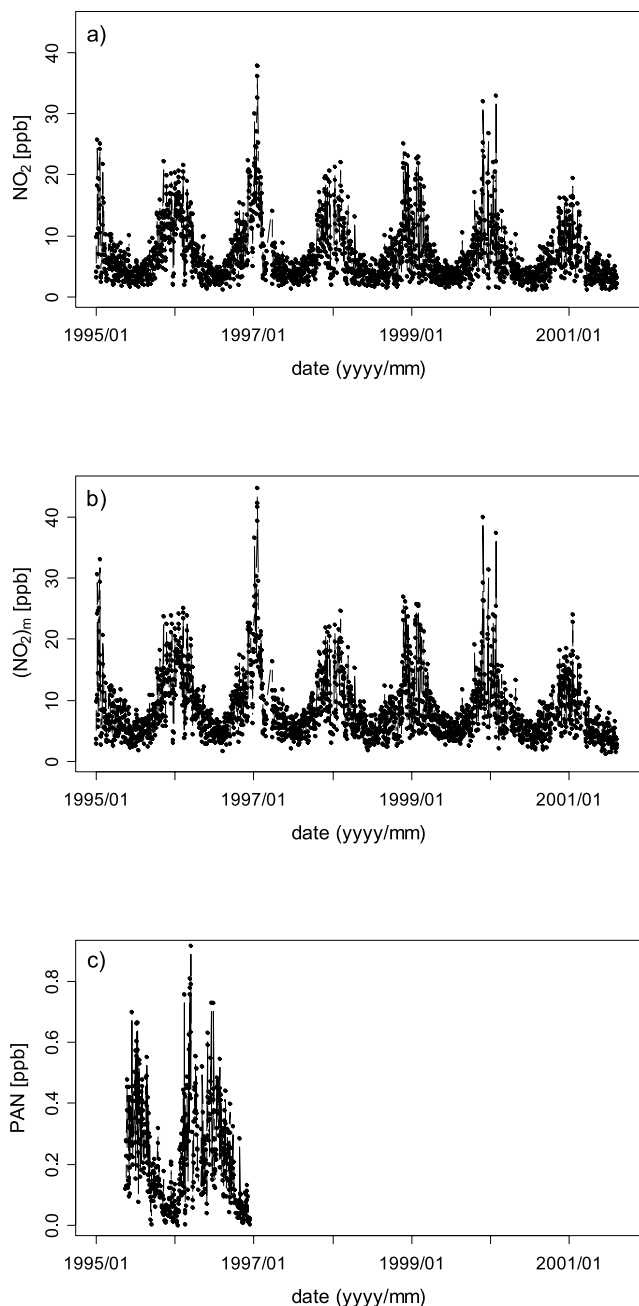


Figure 1. Time series of daily averages of (a) NO_2 measured with photolysis converter, (b) NO_2 measured with molybdenum converter ($\text{NO}_2)_m$, and (c) PAN at Taenikon.

[21] Polytetrafluoroethylene (PTFE) inlet filters ($5 \mu\text{m}$; Whatman-Schleicher and Schuell, Switzerland) were installed indoors at the inlet ports of the instruments to protect the instruments from particulate matter. The inlet filters were changed each 2 weeks during the regular maintenance visits.

[22] Simultaneous NO_2 measurements with both converter techniques are available from January 1995 to August 2001 at Taenikon and from November 2001 to December 2005 at Rigi. PAN measurements were performed at Taenikon from April 1995 to November 1996. Daily samples of total inorganic nitrate are available from January

2000 until today at Rigi. One-hour averages (except for total nitrate) and data until end of 2005 were considered for this work. All data were removed for the analysis when either one of the NO_2 measurements was unavailable. Additionally, the data set was reduced by eliminating the highest and lowest 0.5% of the NO_2/NO_2 ratios to avoid a bias due to extreme NO_2/NO_2 ratios originating from very low NO_2 concentrations.

[23] Parallel to the NO_2 measurements with a molybdenum converter, a Horiba APNA 360 NO_x monitor equipped with a photolytic converter (BLC blue light converter, Droplet Measurement Technologies, Boulder, USA) was installed at Payerne end of January 2006. Measurement uncertainties for 1-h averages are in the same range as for the surface converter instruments. The data for the first half of 2006 were used for validation of the calculated correction factors at Taenikon.

2.3. Calculation of Gas-Particle Partitioning of Total Nitrate

[24] The inorganic aerosol thermodynamic equilibrium model ISORROPIA [Nenes *et al.*, 1998, 1999] was applied to calculate the partitioning of nitrate between the gas and aerosol phases within the sodium-ammonium-chloride-sulphate-nitrate-water system. Daily measurements of total nitrate as well as daily values of total ammonium (sum of particulate ammonium and gaseous ammonia), total sulphate, relative humidity, and ambient temperature were used as input parameters. The concentrations of total sodium and total chlorine were not available but assumed to be negligible and therefore set to zero. Figure 5 shows the annual cycles for the measured total nitrate and calculated gaseous HNO_3 at the Rigi site.

3. Results and Discussion

3.1. Time Series

[25] Figures 1 and 2 show the available data sets from Taenikon and Rigi, respectively. A distinct seasonal cycle with summertime minima at both stations is observed for NO_2 confirmed by both measurement techniques. This is expected because low wind speed, temperature inversion, and most of all a shallow stable boundary layer favor episodes with elevated NO_2 mixing ratios during winter [see, e.g., Munger *et al.*, 1996]. The average daily maximum NO_2 mixing ratio at Taenikon was 37.8 ppb measured with the photolysis converter (NO_2) and 44.8 ppb measured with molybdenum converter ($\text{NO}_2)_m$. Mean mixing ratios are 6.9 ppb for NO_2 and 8.6 ppb for $\text{NO}_2)_m$. At Rigi, daily average maxima of 16.3 ppb for NO_2 and 19.2 ppb for $\text{NO}_2)_m$ and mean values of 2.5 ppb for NO_2 and 4.2 ppb for $\text{NO}_2)_m$ were observed. The lower NO_2 mixing ratios are reflecting the larger distance from NO_x -emission sources. Especially in winter, Rigi is often located above the boundary layer resulting in periods with NO_2 concentrations nearly as low as in summer. Therefore a larger variability of the daily average NO_2 concentrations is observed at Rigi compared with Taenikon in wintertime.

[26] The concentrations at both stations are usually below the Swiss national air quality standards for NO_2 of $80 \mu\text{g}/\text{m}^3$ (approximately 42.5 ppb) for the 24-h mean value. The annual mean air quality standard in Switzerland is $30 \mu\text{g}/\text{m}^3$

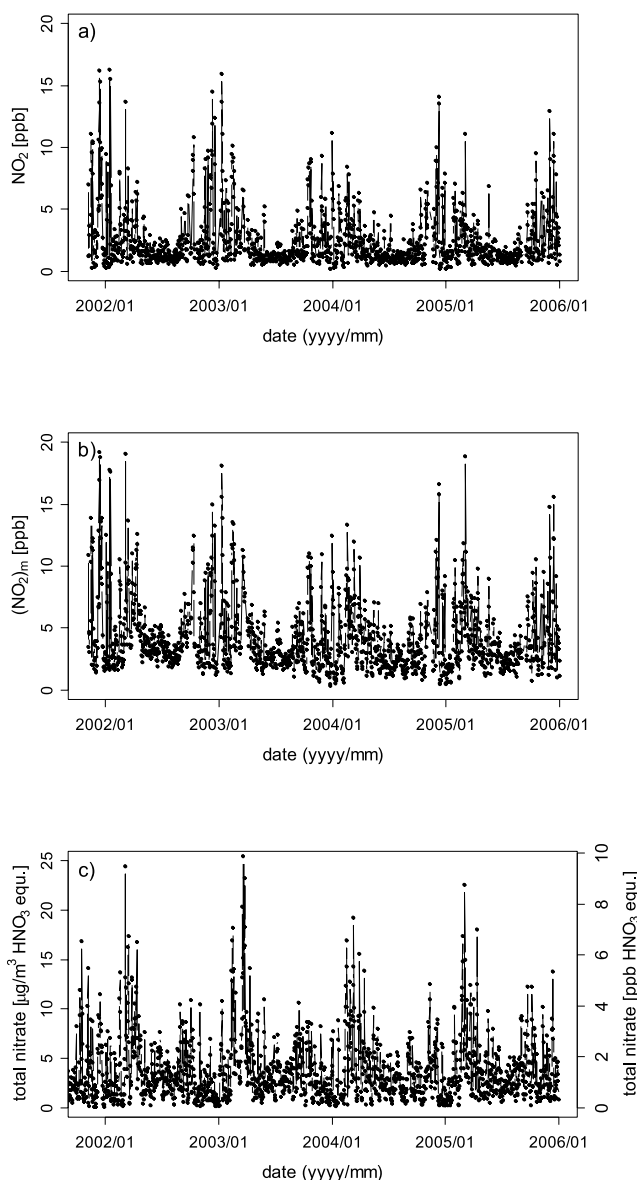


Figure 2. Time series of daily averages of (a) NO_2 measured with photolysis converter, (b) NO_2 measured with molybdenum converter ($\text{NO}_2)_m$, and (c) the sum particulate nitrate and gaseous HNO_3 (total nitrate) at Rigi.

(approximately 16 ppb). However, even at rural sampling sites, exceedances of the NO_2 levels can happen, and thus the number of exceedances depends on the applied measurement technique. Figures 1 and 2 reveal that $(\text{NO}_2)_m$ mixing ratios are higher compared with NO_2 during both pollution events and background conditions.

[27] The time series of PAN mixing ratios at Taenikon (Figure 1c) shows the expected annual cycle with enhanced levels in spring and summer and low mixing ratios in winter (see also Figure 4a). Maximum daily average and mean mixing ratios of 0.9 ppb and 0.2 ppb were observed for the investigated period. A distinct diurnal cycle with highest mixing ratios in the afternoon exists especially in summer, and 1-h average mixing ratios reach up to 1.3 ppb. Consequently, PAN interference is of importance at least during the warm seasons.

[28] The time series of total nitrate at Rigi is presented in Figure 2c. The highest concentrations were measured in spring and autumn. The concentrations in winter are usually lower because of frequent episodes above the boundary layer. The maximum and mean observed concentrations are 25 and $3.7 \mu\text{g}/\text{m}^3$. As discussed below, total nitrate might also contribute significantly to the overestimated $(\text{NO}_2)_m$ signal in all seasons. The seasonal cycles of NO_2 , $(\text{NO}_2)_m$, and total nitrate are presented in Figures 4 and 5, and will be discussed in more detail in section 3.3.

[29] As already mentioned above, HONO might be a potential interference for photolytic converters. Since HONO mixing ratios are usually very low during the day because of rapid photolysis, no significant interference is expected during daytime. Typical nighttime mixing ratios reported for the Alpine region range from about 0.5 ppb at a rural site in southern Switzerland [Staffelbach et al., 1997] and about 1.5 ppb in Zurich [Fisseha et al., 2006], to 2–3 ppb in suburban Zurich [Zellweger et al., 1999] and 2 ppb in Milan, Italy [Stutz et al., 2002]. Acker et al. [2006b] observed higher HONO concentrations during the day than during the night at Hohenpeissenberg, a rural mountain site in Southern Germany similar to the Rigi site. Mixing ratios ranged from about 30 ppt during the night to 100 ppt during the day. Considering the above mentioned conversion efficiency of 20–30%, the nocturnal contribution due to HONO interference amounts to less than 10% of the NO_2 concentration.

3.2. Case Study

[30] Figure 3 presents a case study of a high-pressure period at Taenikon in July 1996. It illustrates the increasing $(\text{NO}_2)_m$ to NO_2 difference (ΔNO_2) with proceeding fair weather. As a result, photochemically produced compounds such as PAN and O_3 build up during the daytime leading to a pronounced diurnal cycle. The molybdenum converter instrument overestimates the NO_2 mixing ratio especially in the afternoon confirmed by high ΔNO_2 and in particular high $(\text{NO}_2)_m/\text{NO}_2$ ratios. These periods coincide with the highest PAN mixing ratios observed in the afternoon. Comparing the daily cycles and absolute levels of ΔNO_2 and PAN during this fair-weather period, we can roughly estimate that 30 to 50% of the ΔNO_2 can be attributed to PAN assuming a PAN to NO conversion efficiency of 100%. PAN was already proposed to cause high NO_y levels at a rural site in New Zealand in the 1980s [Stedman and McEwan, 1983]. However, the greater part of ΔNO_2 at Taenikon cannot be explained by PAN interference. Since a ΔNO_2 of about 1 ppb was already observed at the beginning of the presented period (when PAN was about 0.2 ppb) and ΔNO_2 still slightly increased from 12 to 15 July when PAN levels stagnated, the general offset and the steady increase might be attributed to an interference due to potential losses and memory effects of HNO_3 in the inlet system. The present inlet setup is designed for less reactive gases and includes Ematal-coated aluminum, glass, and PFA Teflon tubes. Therefore it is not well suited for HNO_3 and especially inappropriate for conditions with changing HNO_3 levels as it was the case during the presented period because of strong photochemical production. Neuman et al. [1999] recommended the use of Teflon for the sample lines but reported considerable HNO_3

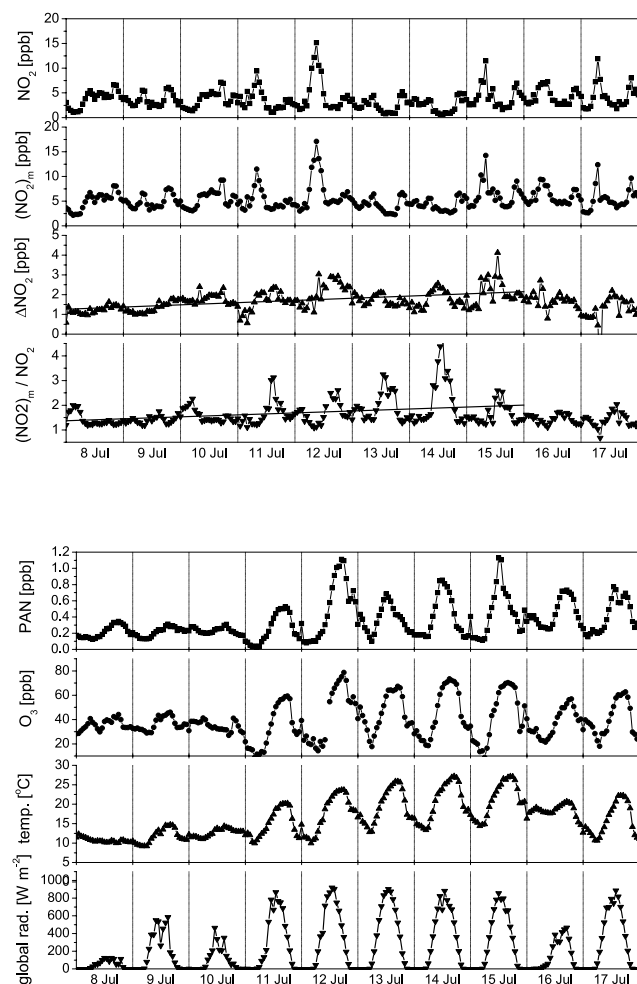


Figure 3. Ten-day case study showing the time series of NO_2 , $(\text{NO}_2)_m$, ΔNO_2 , $(\text{NO}_2)_m/\text{NO}_2$, PAN, O_3 , temperature, and global radiation at Taenikon during a fair-weather period in July 1996. Linear fits are added for ΔNO_2 and $(\text{NO}_2)_m/\text{NO}_2$ illustrating the positive trend of these two parameters for the period from 8 July to 16 July.

adsorption on glass in the beginning of the exposure followed by a passivation within hours of continuous exposure to HNO_3 . Therefore they recommend glass tubes only for conditions with constant HNO_3 concentrations and sufficient exposure times because of severe memory effects. In good agreement with our study, Grosjean [1983] calculated overestimates of the “real” NO_2 of up to 65% assuming a 100% conversion of PAN and HNO_3 to NO 45 km downwind of Los Angeles in 1980. No HNO_3 data were available for Taenikon. HNO_3 concentrations at Rigi derived from the total nitrate filter samples are presented in Figure 5. Literature data of simultaneous measurements of PAN and HNO_3 show significantly higher (about double) HNO_3 than PAN mixing ratios at an urban background station in Rome in May/June 2001 [Acker et al., 2006a], on average slightly higher HNO_3 levels in the suburbs of Nashville, USA in June/July 1994 [Williams et al., 1998], and similar PAN and HNO_3 concentrations in southern Switzerland in summer 1994 [Staffelbach et al., 1997]. Similar PAN and HNO_3 concentrations were also observed

by Murphy et al. [2006] at an elevated station and a suburban site in the Sacramento area, USA in summer 2001. HNO_3 mixing ratios up to 4 ppb were reported about 30 km of Marseille, France in summer 2001 [Acker et al., 2005]. Hayden et al. [2003] investigated the partitioning of the major reactive nitrogen species at an elevated site in Canada. PAN and HNO_3 contributed to the total reactive nitrogen with 9 and 18% in winter and 13 and 20–25% in summer, respectively.

[31] Particulate nitrate might affect the measurements because it can be adsorbed on the inlet filter of the instrument. Subsequent evaporation of the particulate nitrate and a passage through the filter that in turn interferes with the NO_2 measurements cannot be excluded. However, particulate nitrate concentrations are usually lower during the warm season, so that the effect might be of minor importance for the presented period.

[32] The observed daily cycle and the trends of ΔNO_2 and $(\text{NO}_2)_m/\text{NO}_2$ during this fair-weather period reveal that local and/or regional photochemical production of NO_x oxidation products ($\equiv \text{NO}_z = \text{NO}_y - \text{NO}_x$) can considerably influence the level of interference. Consequently, the degree of overestimation depends on transport processes as well as on the local photochemical and meteorological conditions. This is clearly seen comparing the daily maxima of ΔNO_2 and $(\text{NO}_2)_m/\text{NO}_2$ in the afternoon with the daily PAN cycle. Mean yearly cycles of the $(\text{NO}_2)_m/\text{NO}_2$ ratio (see section 3.3) are appropriate for a first correction of the data [similarly as done by Ordóñez et al. [2006] and Schaub et al. [2006] for the times of the Global Ozone Monitoring Experiment (GOME) overpass]. A more detailed analysis by means of a multiple linear regression (see section 3.4) can be useful for a more elaborate consideration.

3.3. Yearly and Diurnal Cycles

[33] Regarding annual cycles (Figure 4), ΔNO_2 at Taenikon is highest in winter (when NO_2 concentrations are highest) and spring, whereas ΔNO_2 maxima were observed at Rigi in spring. The phenomenon in spring is similar to the frequently observed spring O_3 maxima at elevated sites that are at least partially of photochemical origin [see, e.g., Brönnimann, 1999; Monks, 2000] and correlates well with the observed annual cycle of PAN at Taenikon as well as with enhanced NO_y levels at the high alpine site Jungfraujoch (3580 m asl) [Zanis et al., 2007]. Hayden et al. [2003] investigated the partitioning of the major reactive nitrogen compounds in a rural hilly area in Canada. They compared total NO_y measurements with the sum of individual NO , NO_2 , HNO_3 , and PAN measurements and reported a NO_y deficit (often called “missing NO_y ”). The early spring maximum of the NO_y deficit remained unexplained. Numerous other studies that compared total NO_y measurements with the sum of individual species also reported missing NO_y [see Roberts, 1995 and references therein; Harrison et al., 1999; Zellweger et al., 2000] and attributed it mostly to organic nitrates. Recently, Day et al. [2003] and Murphy et al. [2006], who individually measured total alkyl nitrates by thermal dissociation laser-induced fluorescence, found that a large part of the missing NO_y can be attributed to alkyl nitrates.

[34] The discrepancy between the measurements of NO_2 in winter may be at least partly attributed to particulate

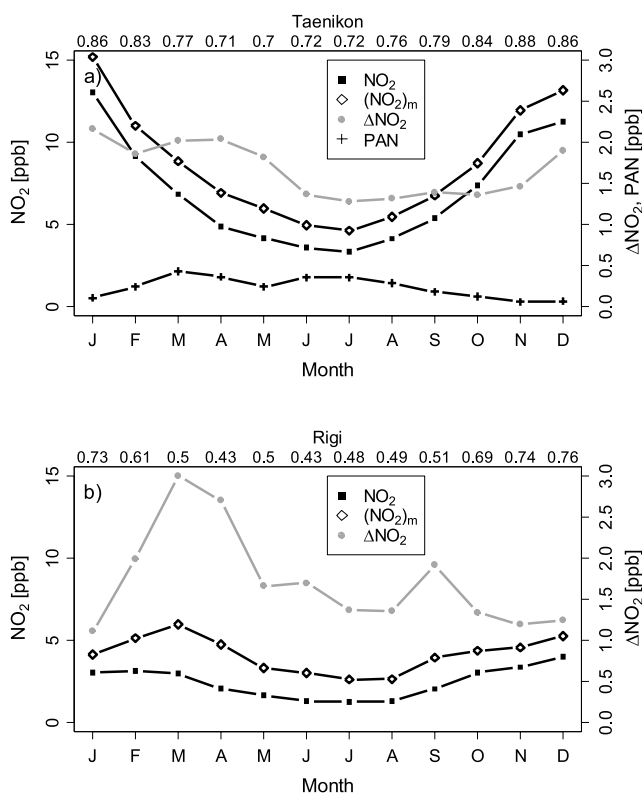


Figure 4. Annual cycles of (a) NO_2 and $(\text{NO}_2)_m$, ΔNO_2 , and PAN at Taenikon and (b) of NO_2 and $(\text{NO}_2)_m$ and ΔNO_2 at Rigi. Scaling is different for ΔNO_2 and PAN. Numbers on top denote the monthly mean $\text{NO}_2/(\text{NO}_2)_m$ ratios.

nitrate (p-NO_3^-). As already mentioned, a PTFE inlet filter is installed at the inlet port of the instruments to protect the instrument from particulate matter. Adsorbed particles can evaporate from the inlet filter, resulting in a potential positive interference. Indoor-outdoor temperature differences result in different gas-particle partitioning with gaseous species being favored in warmer air. During the warm seasons, particulate nitrate concentrations are usually lower (see Figure 5), and the temperature difference between indoor and outdoor air is significantly smaller, so that evaporation of particulate nitrate will be negligible. The observed mean annual cycle of total nitrate (p-NO_3^- plus gaseous HNO_3) as well as gaseous HNO_3 calculated with the inorganic thermodynamic model ISORROPIA are illustrated for Rigi in Figure 5. A pronounced maximum of total nitrate at Rigi is observed in spring that is mostly attributed to p-NO_3^- since the total nitrate maximum coincides with a HNO_3 minimum. *Munger et al.* [1996] reported for a forested sampling site in Canada that the particulate nitrate accounted for 16–40% of the total nitrate signal throughout the year. Our calculations resulted in contributions of particulate nitrate to total nitrate at Rigi between 40% in July and 88% in March, resulting in an annual mean contribution of 65%. Measurements of gaseous HNO_3 and particulate nitrate made with a wet effluent diffusion denuder/aerosol collector at another NABEL site (Zurich) from August to September 2002 and in March 2003 revealed monthly mean HNO_3 to total nitrate ratios of

approximately 10, 55, and 25% for March, August, and September, respectively [Fisseha et al., 2006]. This is in good agreement with our HNO_3 -to-total nitrate ratios listed on top of Figure 5.

[35] Daily averages of ΔNO_2 correlate well with total nitrate daily data. The correlation exhibits similar coefficients of determination ($R^2 = 0.61$ to 0.72) as well as comparable slopes of 0.35 to 0.4 ΔNO_2 per total nitrate for all seasons. The importance of particulate nitrate and gaseous nitrogen species for the observed ΔNO_2 can be studied when looking at the ISORROPIA outputs; highest coefficients of determination ($R^2 = 0.63$) between ΔNO_2 and p-NO_3^- were observed in winter and spring when ΔNO_2 as well as p-NO_3^- cover a larger concentration range. Poor ΔNO_2 -to- HNO_3 correlations ($R^2 = 0.06$ to 0.25) were observed for all seasons. The above mentioned memory effects related to HNO_3 and uncertainties of the HNO_3 determination with the equilibrium model might blur the interfering effect of nitric acid and makes it only hardly detectable. Additionally, long-range transport, photochemical conditions and oxidation capacity of the atmosphere, atmospheric stability, and the contribution of single compounds are highly variable within 1 day and throughout the whole year, resulting in highly variable total nitrate data, so that interannual variations cannot be clearly detected.

[36] Further conclusions can be drawn when analyzing $(\text{NO}_2)_m/\text{NO}_2$ ratios (see Figure 6). Generally, lower $(\text{NO}_2)_m/\text{NO}_2$ ratios were observed in fall and winter at both stations. $(\text{NO}_2)_m/\text{NO}_2$ ratios show only small diurnal variations when using molybdenum converter instruments, true NO_2 concentrations are more overestimated in spring and summer illustrated by higher $(\text{NO}_2)_m/\text{NO}_2$ ratios. These ratios also show a distinct diurnal cycle reflecting the more prevalent photochemistry when solar input is higher with ratios between 1.4 and 1.8 in spring and 1.2 to 1.8 in summer. Lowest $(\text{NO}_2)_m/\text{NO}_2$ ratios at Taenikon were always observed in the morning representing fresh emissions and highest ratios in the afternoon when the air masses are more photochemically aged.

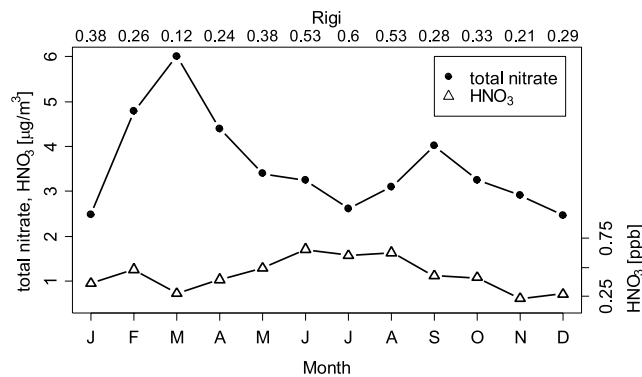


Figure 5. Annual cycles of total nitrate (impregnated filter measurements) and gaseous HNO_3 (calculated with ISORROPIA) at Rigi. The difference between the two curves is attributed to particulate nitrate. Numbers on top denote the HNO_3 to total nitrate ratios.

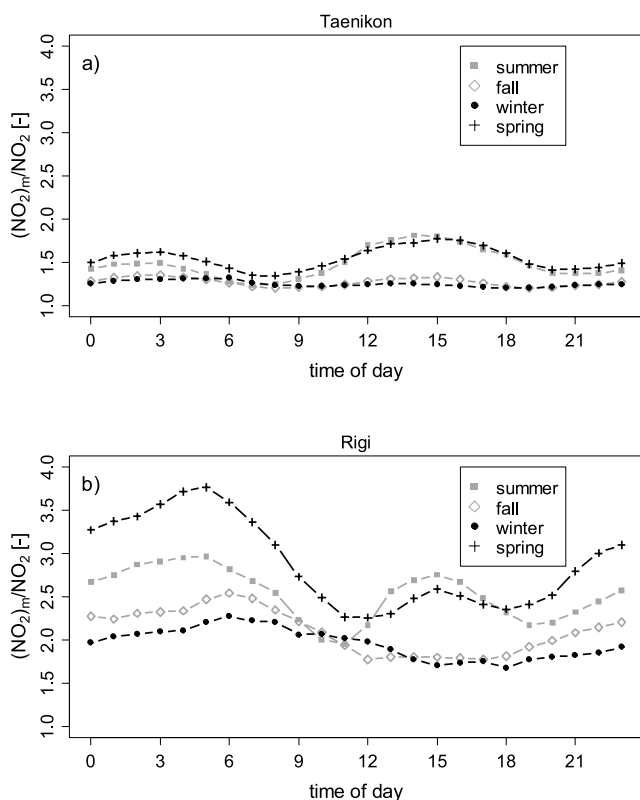


Figure 6. Diurnal cycles of $(\text{NO}_2)_m/\text{NO}_2$ at (a) Taenikon and (b) Rigi. Each season is presented separately.

[37] $(\text{NO}_2)_m/\text{NO}_2$ ratios are generally higher at Rigi because this site is further away from pollution sources. However, similar patterns were observed at both stations. Less pronounced diurnal cycles were also monitored at Rigi during the cold seasons (1.8 to 2.5 and 1.7 to 2.3 in fall and winter, respectively). Considerable diurnal cycles were detected for the other seasons (2.3 to 3.8 in spring and 2.0 to 3.0 in summer). The morning minimum appears later compared with Taenikon when up-valley winds with boundary-layer air reach the sampling site. It is noteworthy that during the night, when residual layer air is measured, $(\text{NO}_2)_m/\text{NO}_2$ ratios between 2 and 2.5 were observed in fall and winter. Nighttime ratios between 2.5 and 3 were detected in summer, and ratios higher than 3 were measured in spring. These findings clearly demonstrate that data of molybdenum converter instruments need to be corrected for the overestimation by interfering compounds, especially at rural and remote sites. Since the concentrations at these sites are usually low, the overestimation is not of major concern for air quality issues, i.e., violations of the air quality limits. However, the interference has to be considered when using the data as input parameters for air-quality modeling, model-measurement intercomparisons, or the validation of satellite data. Lower temperatures usually prevail at Rigi because of its higher altitude compared to Taenikon. This fact could also favor higher $(\text{NO}_2)_m/\text{NO}_2$ ratios due to the temperature-dependent gas-particle partitioning but is not expected to be of major importance. Finally, it should be kept in mind that the data discussed in this section are monthly and hourly averages. During specific periods,

$(\text{NO}_2)_m/\text{NO}_2$ ratios can even reach considerably higher values (as shown in Figure 3).

3.4. Modeling ΔNO_2 Using Multiple Linear Regression

[38] For a first approximation, monthly averaged $(\text{NO}_2)_m/\text{NO}_2$ ratios similar as used by Ordóñez *et al.* [2006] for the times of the GOME overpasses are proved to be a useful approach to correct the measured $(\text{NO}_2)_m$ concentrations. They showed that the agreement of in situ measurements with tropospheric NO_2 concentrations derived from satellite data improved by applying a correction based on monthly $\text{NO}_2/(\text{NO}_2)_m$ ratios. Our attempt was to refine the correction of $(\text{NO}_2)_m$ in order to obtain unbiased NO_2 mixing ratios. The linear regression model was kept as simple as possible to enable a correction for most monitoring sites equipped with standard instrumentation. Therefore only a small set of the available variables was chosen as independent predictors. Initially, an extended set of variables was selected. Subsequently, more and more variables were excluded as long as the explained fraction of the variance did not decrease by more than 0.5 and 0.3% at Taenikon and Rigi. Finally, we kept only the NO_2 measured with the molybdenum converter $(\text{NO}_2)_m$, the O_3 mixing ratio as an indicator for photochemical activity, as well as the factorized predictors month and (day/night). The factor (day/night) is a binary predictor distinguishing between day and night conditions with the value 1 and 0 when the 1-h averaged global radiation was above and below 5 W/m^2 , respectively. If no global radiation data are available, this variable can also be generated on the basis of the time of the day. Thus our multiple linear model has the following form:

$$\Delta\text{NO}_2 = a \cdot (\text{NO}_2)_m + b \cdot \text{O}_3 + c \cdot \text{factor}(\text{month}) + d \cdot \text{factor}(\text{day/night}) + e + \varepsilon \quad (1)$$

with the above mentioned variables $(\text{NO}_2)_m$, O_3 , month, (day/night), and the coefficients of the variables a to d , an intercept e , and a residual ε . The results of the linear regressions for Rigi and Taenikon are listed in Table 1. The linear models explain 34 and 59% of the variance of the observed ΔNO_2 at Taenikon and Rigi, respectively. The lower value at Taenikon occurs because of the larger variance of the measured NO_2 differences (see Figure 7a and Figure 8a). The coefficients for the individual months generate different offsets for each month and demonstrate a similar general pattern than the observed ΔNO_2 (compare Table 1 with Figure 4). These coefficients fit the modeled monthly means of ΔNO_2 to the observed ones, so that the annual cycles for $\Delta\text{NO}_{2,\text{modelled}}$ and $\Delta\text{NO}_{2,\text{measured}}$ perfectly match (not shown here). The diurnal cycles that are illustrated in Figure 9 reveal that the diurnal cycles also agree very well at Taenikon and reasonably well at Rigi. Because of the more demanding conditions at Rigi with upslope transport of polluted air masses during the afternoon and conditions when the sampling site is above the boundary layer and photochemically aged air masses are sampled, a suboptimal agreement was expected. The observed ΔNO_2 is satisfactorily modeled as shown in Figure 8a where the time series of $\Delta\text{NO}_{2,\text{modelled}}$ and $\Delta\text{NO}_{2,\text{measured}}$ are displayed for the whole year 2002. Nevertheless, the model is not capable of reproducing all short-term

Table 1. Results of the Multiple Linear Regression Model for Taenikon and Rigi^a

Variables	Coefficient	
	Taenikon	Rigi
Intercept (<i>e</i>)	-1.32E-1	-1.16
(NO ₂) _m (<i>a</i>)	1.32E-1	2.57E-1
O ₃ (<i>b</i>)	2.71E-2	3.66E-2
Month (<i>c</i>)		
Jan	0	0
Feb	-0.012	0.464
Mar	0.258	1.086
Apr	0.380	0.912
May	0.239	0.244
Jun	-0.092	0.0136
Jul	-0.105	0.014
Aug	-0.135	0.016
Sep	0.050	0.592
Oct	-0.050	0.303
Nov	-0.274	0.151
Dec	-0.026	0.041
(Day/night): day (<i>d</i>)	-1.87E-1	-1.52E-1
(Day/night): night	0	0
R ²	0.34	0.59

^aNotation of the coefficients according to equation (1).

variability. This is also corroborated by Figure 8b, which exemplarily illustrates the results of a selected 10-day period at Rigi in July 2002. Even so, the correction leads to a good general agreement between calculated NO₂ ((NO₂)_{calc}) and NO₂ for the same 10-day period (Figure 8c). The largest differences between (NO₂)_{calc} and NO₂ appear for low NO₂.

[39] A similar pattern also holds for Taenikon where the majority of the ΔNO_2 is nicely reproduced by the model, and only the outliers cannot be simulated (see Figure 7a for the whole year 1996 and Figure 7b for a selected 10-day period in July 1996). The direct (NO₂)_{calc}-to-NO₂ comparison (Figure 7c) shows nearly a perfect match. Generally higher NO₂ mixing ratios but ΔNO_2 in the same range at Taenikon as at Rigi result in smaller relative errors between (NO₂)_{calc} and NO₂. Thus the correction at Taenikon led to a very good agreement.

[40] Finally we can conclude that the model satisfactorily reproduces mean ΔNO_2 . Also, on a short timescale, the agreement is usually very good even if the model cannot simulate all observed variability. The $\Delta\text{NO}_{2,\text{modelled}}$ -to- $\Delta\text{NO}_{2,\text{measured}}$ agreement is better at Rigi since observations show less short timescale variability. When applying $\Delta\text{NO}_{2,\text{modelled}}$ to (NO₂)_m to calculate the corrected NO₂ data and comparing them with NO₂, the higher NO₂ levels at Taenikon result in smaller relative differences at this sampling site.

[41] We also applied a similar model to predict the NO₂ mixing ratios by means of the NOO₃ product, the O₃ mixing ratio, and the factorized predictors “month” and “day/night”. This approach is based on considerations of the photostationary steady state. It explains more of the variance than model (1) at Taenikon but less at Rigi and especially suffers from negative mixing ratios at both stations in summer, which makes it unemployable. This might be due to the experimental (relative) uncertainties in the measurement of NO, which are particularly high in summer as a consequence of the low NO levels in this

season. Moreover, recent studies at rural sites in Central Europe revealed significant deviations from the photostationary steady state at nonelevated [Volz-Thomas *et al.*, 2003] as well as elevated sites [Mannschreck *et al.*, 2004].

3.5. Applications for Measurements in the Troposphere

[42] The multiple linear model approach presented in the previous section aimed at providing a tool to estimate the real NO₂ mixing ratios also for other rural and rural-elevated sites in Central Europe. As a first independent test, we applied our results (i.e., the coefficients *a* to *e*) obtained for Taenikon to the (NO₂)_m at Payerne and compared the results with the mixing ratios measured with the blue light (photolytic) converter. Figure 10 reveals the monthly averaged measured (NO₂)_m and NO₂ mixing ratios as well as the

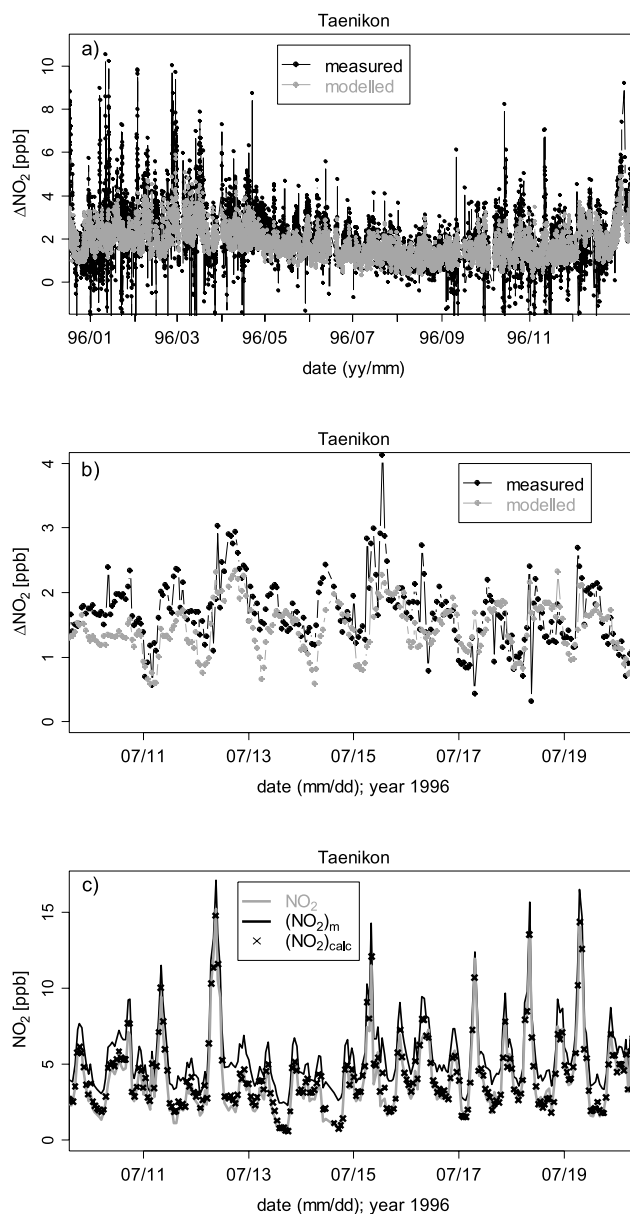


Figure 7. Time series of measured and modeled ΔNO_2 at Taenikon (a) for 1996 and (b) for a 10-day period in July 1996 and (c) (NO₂)_m, NO₂, and calculated NO₂ (NO₂)_{calc} for the same period.

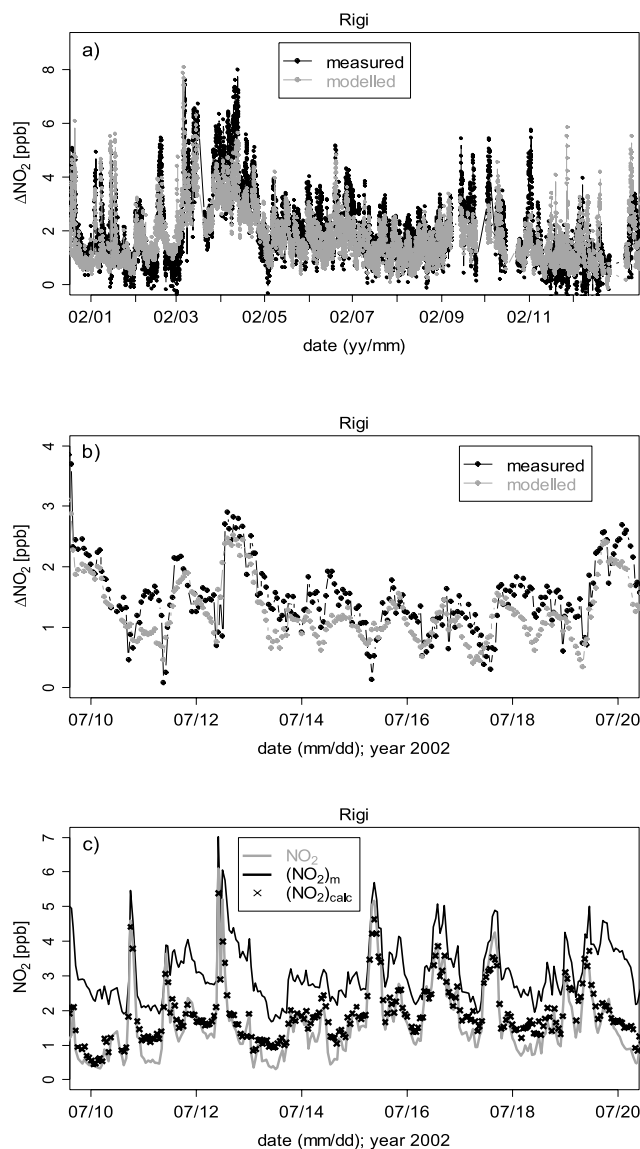


Figure 8. Time series of measured and modeled ΔNO_2 at Rigi (a) for 2002, (b) for a 10-day period in July 2002, and (c) $(\text{NO}_2)_m$, NO_2 , and calculated NO_2 $(\text{NO}_2)_{calc}$ for the same period.

calculated NO_2 by means of the Taenikon model approach. The comparison demonstrates an excellent agreement and confirms the applicability of our approach to stations in a similar environment.

[43] However, the direct adaptability of the present analysis to other sampling sites has to be done with caution. The correction should preferably be applied to a station with similar characteristics. Taenikon might act as a representative station for a rural sampling site whereas Rigi is a rural elevated site, both in Central Europe. For a first indication which correction to apply, the user might look at the mean measured mixing ratios. At Taenikon, we observed 3.9 ppb NO , 8.6 ppb $(\text{NO}_2)_m$, and 12.4 ppb $(\text{NO}_x)_m$. The respective numbers for Rigi are 0.4 ppb NO , 4.2 ppb $(\text{NO}_2)_m$, and 4.6 ppb $(\text{NO}_x)_m$. Even for similar environmental conditions (rural or elevated rural sites, similar latitudes, similar meteorological and climatological conditions), the losses

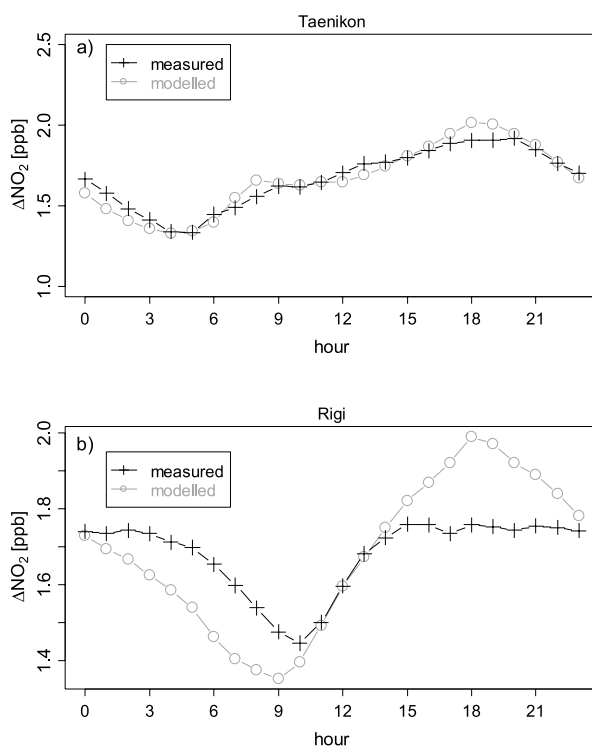


Figure 9. Measured and modeled diurnal cycles of ΔNO_2 at (a) Taenikon and (b) Rigi.

of NO_2 species in the inlet line are the most crucial uncertainty factor. Since the losses due to adsorption on the tubing walls are temperature- and material-dependent [Neuman *et al.*, 1999], the temperature in the station as well as used materials can alter the recovery rates of HNO_3 and subsequently the NO_2 ratios observed with surface and photolytic converters. Inlet system and inlet filter phenomena are difficult to quantify and are not considered in the multiple linear model. Nevertheless, the present analysis using a unique perennial data set of collocated measurements with both converter types provides a first approxi-

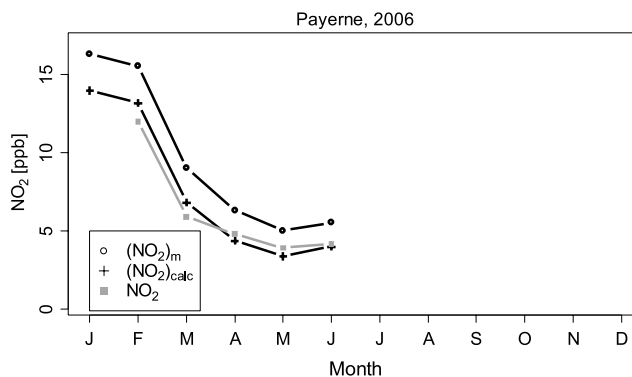


Figure 10. Monthly mean NO_2 mixing ratios at Payerne in 2006 measured with a molybdenum converter instrument $(\text{NO}_2)_m$ and a photolytic (blue light) converter instrument NO_2 and the calculated NO_2 mixing ratios $(\text{NO}_2)_{calc}$ when applying the results of the multiple linear model for Taenikon.

mation estimate of how much instruments with surface converters are overestimating the real NO₂ levels.

4. Conclusions

[44] Perennial measurements of NO₂ with two different converter techniques at two rural sites in Switzerland showed that the commonly used NO₂ instruments equipped with surface (molybdenum) converters to reduce NO₂ to NO are also significantly overestimating the real NO₂ concentrations under ambient air conditions. Mean (NO₂)_m/NO₂ ratios of about 1.5 at Taenikon and up to 3.5 at Rigi emphasize the need to take those interferences into account. In other words, on a monthly basis, only 70 to 83% of the measured (NO₂)_m can be attributed to real NO₂ at Taenikon and even less (43 to 76%) at Rigi (see top lines in Figure 4).

[45] We showed by means of a case study that changing meteorological conditions can vary the degree of overestimation within the range of hours to days. In summer, PAN and HNO₃ are most probably the dominating interfering species. The quantification is difficult especially for HNO₃ as it is known to be deposited in the inlet system. Derived HNO₃ concentrations from filter samples under the consideration of chemical equilibrium did not show a considerably better agreement with the observed interferences in summer than in winter. This might be related to a blurring of the effect due to the above mentioned memory effects.

[46] Despite the sampling artifacts, the multiple linear model yielded convincing results for both sampling sites. Only (NO₂)_m, O₃, a coefficient representing the mean annual pattern, and a binary daytime-nighttime consideration were implemented in the model to keep it as simple as possible to enable the application to other continuously operated measurement sites. The first application to another sampling site revealed very promising results even if it has to be considered that the inlet set-up is identical for both sites.

[47] The transferability to other stations in similar environments is therefore generally possible, but it should be taken into account that the losses of HNO₃ in different parts of the inlet system are not quantified. Other inlet configurations may have other adsorption characteristics which can influence the results. However, the present unique data set provides a good basis to study the bias of NO₂ concentrations measured with surface converters depending on season and meteorological and chemical parameters.

[48] Finally, it should be mentioned that the “Ambient air quality-Standard method for the measurement of the concentration of nitrogen dioxide and nitrogen monoxide by chemiluminescence in Europe (EN 14211:2005)” is restricted to heated furnace converters made of stainless steel, copper, molybdenum, tungsten, or carbon with converter efficiencies of at least 95%. Because most of the continuous observations are conducted on behalf of the environmental offices that are in turn obliged to follow the European standard, surface converter instruments will be also used in future. Since the performance of photolytic converters improved considerably and a number of other techniques became available in the last years, it should be considered to use artifact-free instruments for long-term monitoring and climate-relevant issues. However, new emerging tech-

niques have still to prove their long-term applicability. The US Environmental Protection Agency (EPA) recommends using alternative measuring methods in geographical areas where considerable interferences from surface converters can be expected [*Environmental Protection Agency (EPA)*, 2007]. The influence on numbers of NO₂ air quality violations should be small since most violations are observed in urban environments close to NO_x sources where NO₂ concentrations are high, and the amount of oxidized nitrogen compounds other than NO_x is rather small. However, molybdenum converter NO₂ measurements represent an upper limit NO₂ concentration even at such polluted sites. More frequent use of artifact-free instruments would especially improve the availability of reliable data for the validation of results retrieved from satellite observations and chemical transport models.

[49] **Acknowledgments.** This research was carried out under the financial support of the Swiss Federal Office for the Environment (FOEN).

References

- Acker, K., D. Möller, R. Auel, W. Wieprecht, and D. Kalass (2005), Concentrations of nitrous acid, nitric acid and nitrate in the gas and aerosol phase at a site in the emission zone during ESCOMPTE 2001 experiment, *Atmos. Res.*, *74*, 507–524.
- Acker, K., A. Febo, S. Trick, C. Perrino, P. Bruno, P. Wiesen, D. Möller, W. Wieprecht, R. Auel, M. Giusto, A. Geyer, U. Platt, and I. Allegrini (2006a), Nitrous acid in the urban area of Rome, *Atmos. Environ.*, *40*, 3123–3133.
- Acker, K., D. Möller, W. Wieprecht, F. X. Meixner, B. Bohn, S. Gilge, C. Plass-Dülmer, and H. Berresheim (2006b), Strong daytime production of OH from HNO₂ at a rural mountain site, *Geophys. Res. Lett.*, *33*, L02809, doi:10.1029/2005GL024643.
- Alicke, B., U. Platt, and J. Stutz (2002), Impact of nitrous acid photolysis on the total hydroxyl radical budget during the Limitation of Oxidant Production/Pianura Padana Produzione di Ozono study in Milan, *J. Geophys. Res.*, *107*(D22), 8196, doi:10.1029/2000JD000075.
- Brönnimann, S. (1999), Early spring ozone episodes: Occurrence and case study, *Phys. Chem. Earth (C)*, *24*, 531–536.
- Brunner, D., J. Staehelin, D. Jeker, H. Wernli, and U. Schumann (2001), Nitrogen oxides and ozone in the tropopause region of the Northern Hemisphere: Measurements from commercial aircraft in 1995/1996 and 1997, *J. Geophys. Res.*, *106*, 27,673–27,699.
- Cleary, P. A., P. J. Wooldridge, and R. C. Cohen (2002), Laser-induced fluorescence detection of atmospheric NO₂ with a commercial diode laser and a supersonic expansion, *Appl. Opt.*, *41*, 6950–6956.
- Day, D. A., P. J. Wooldridge, M. B. Dillon, J. A. Thornton, and R. C. Cohen (2002), A thermal dissociation laser-induced fluorescence instrument for in-situ detection of NO₂, peroxy nitrates, alkyl nitrates, and HNO₃, *J. Geophys. Res.*, *107*(D6), 4046, doi:10.1029/2001JD000779.
- Day, D. A., M. B. Dillon, P. J. Wooldridge, J. A. Thornton, R. S. Rosen, E. C. Wood, and R. C. Cohen (2003), On alkyl nitrates, O₃, and the “missing NO_y”, *J. Geophys. Res.*, *108*(D16), 4501, doi:10.1029/2003JD003685.
- Donnelly, V. M., D. G. Keil, and F. Kaufman (1979), Fluorescence lifetime studies of NO₂. III. Mechanism of fluorescence quenching, *J. Chem. Phys.*, *71*, 659–673.
- Dunlea, E. J., et al. (2007), Evaluation of nitrogen dioxide chemiluminescence monitors in a polluted urban environment, *Atmos. Chem. Phys. Discuss.*, *7*, 569–604.
- Emmons, L. K., et al. (1997), Climatologies of NO₂ and NO_x: A comparison of data and models, *Atmos. Environ.*, *31*, 1851–1904.
- Environmental Protection Agency (EPA) (2007), Electronic Code of Federal Regulations (e-CFR) of the Clean Air Act Air Regulations 40, Part 50, Appendix F.
- Fahey, D. W., G. Hübler, D. D. Parrish, E. J. Williams, R. B. Norton, B. A. Ridley, H. B. Singh, S. C. Liu, and F. C. Fehsenfeld (1986), Reactive nitrogen species in the troposphere: Measurements of NO, NO₂, HNO₃, particulate nitrate, peroxyacetyl nitrate (PAN), O₃, and total reactive odd nitrogen (NO_y) at Niwot Ridge, Colorado, *J. Geophys. Res.*, *91*, 9781–9793.
- Fehsenfeld, F. C., et al. (1987), A ground-based intercomparison of NO, NO₂, and NO_y measurement techniques, *J. Geophys. Res.*, *92*, 14,710–14,722.

- Fehsenfeld, F. C., D. D. Parrish, and D. W. Fahey (1988), The measurement of NO_x in the non-urban troposphere, in *Tropospheric Ozone*, edited by I. S. A. Isaksen, pp. 185–215, Springer, New York.
- Fehsenfeld, F. C., et al. (1990), Intercomparison of NO_2 measurement techniques, *J. Geophys. Res.*, *95*, 3579–3597.
- Fisseha, R., J. Dommen, L. Gutzwiller, E. Weingartner, M. Gysel, C. Emmenegger, M. Kalberer, and U. Baltensperger (2006), Seasonal and diurnal characteristics of water soluble inorganic compounds in the gas and aerosol phase in the Zurich area, *Atmos. Chem. Phys.*, *6*, 1895–1904.
- Gehrig, R., and R. Baumann (1993), Comparison of 4 different types of commercially available monitors for nitrogen oxides with test gas mixtures of NH_3 , HNO_3 , PAN and VOC in ambient air, paper presented at EMEP Workshop on Measurements of Nitrogen-Containing Compounds, EMEP/CCC Report 1/93, Les Diablerets, Switzerland.
- Gerboles, M., F. Lagler, D. Rembges, and C. Brun (2003), Assessment of uncertainty of NO_2 measurements by the chemiluminescence method and discussion of the quality objective of the NO_2 European Directive, *J. Environ. Monit.*, *5*, 529–540.
- Grosjean, D. (1983), Distribution of atmospheric nitrogenous pollutants at a Los Angeles area smog receptor site, *Environ. Sci. Technol.*, *17*, 13–19.
- Grosjean, D., and J. Harrison (1985), Response of chemiluminescence NO_x analyzers and ultraviolet ozone analyzers to organic air pollutants, *Environ. Sci. Technol.*, *19*, 862–865.
- Harrison, R. M., J. L. F. Grenfell, S. Yamulki, K. C. Clemitshaw, S. A. Penkett, J. N. Cape, and G. G. McFayden (1999), Budget of NO_y species measured at a coastal site, *Atmos. Environ.*, *33*, 4255–4272.
- Hauglustaine, D. A., L. K. Emmons, M. Newchurch, G. P. Brasseur, T. Takao, K. Matsubara, J. Johnson, B. Ridley, J. Stith, and J. Dye (2001), On the role of lightning NO_x in the formation of tropospheric ozone plumes: A global model perspective, *J. Atmos. Chem.*, *38*, 277–294.
- Hayden, K. L., K. G. Anlauf, D. R. Hastie, and J. W. Bottenheim (2003), Partitioning of reactive atmospheric nitrogen oxides at an elevated site in southern Quebec, Canada, *J. Geophys. Res.*, *108*(D19), 4603, doi:10.1029/2002JD003188.
- Henne, S., J. Dommen, B. Neiningner, S. Reimann, J. Stachelin, and A. S. H. Prevot (2005), Influence of mountain venting in the Alps on the ozone chemistry of the lower free troposphere and the European pollution export, *J. Geophys. Res.*, *110*, D22307, doi:10.1029/2005JD005936.
- Jacob, D. J., et al. (1996), Origin of ozone and NO_x in the tropical troposphere: A photochemical analysis of aircraft observations over the South Atlantic basin, *J. Geophys. Res.*, [Atmos.], *101*, 24,235–24,250.
- Jaegle, L., L. Steinberger, R. V. Martin, and K. Chance (2005), Global partitioning of NO_x sources using satellite observations: Relative roles of fossil fuel combustion, biomass burning and soil emissions, *Faraday Discuss.*, *130*, 407–423.
- Kebabian, P. L., S. C. Herndon, and A. Freedman (2005), Detection of nitrogen dioxide by cavity attenuated phase shift spectroscopy, *Anal. Chem.*, *77*, 724–728.
- Kelly, T. J., C. W. Spicer, and G. F. Ward (1990), An assessment of the luminol chemiluminescence technique for measurements of NO_2 in ambient air, *Atmos. Environ.*, *24A*, 2397–2403.
- Kurtenbach, R., K. H. Becker, J. A. G. Gomes, J. Kleffmann, J. Lörzer, M. Spittler, P. Wiesen, R. Ackermann, A. Geyer, and U. Platt (2001), Investigation of emissions and heterogeneous formation of HONO in a road traffic tunnel, *Atmos. Environ.*, *35*, 3385–3394.
- Lee, D. S., I. Kohler, E. Grobler, F. Rohrer, R. Sausen, L. GallardoKlenner, J. G. J. Olivier, F. J. Dentener, and A. F. Bouwman (1997), Estimations of global NO_x emissions and their uncertainties, *Atmos. Environ.*, *31*, 1735–1749.
- Li, Y. Q., K. L. Demerjian, M. S. Zahniser, D. D. Nelson, J. B. McManus, and S. C. Herndon (2004), Measurement of formaldehyde, nitrogen dioxide, and sulfur dioxide at Whiteface Mountain using a dual tunable diode laser system, *J. Geophys. Res.*, *109*, D16S08, doi:10.1029/2003JD004091.
- Mannschreck, K., S. Gilge, C. Plass-Dülmer, W. Fricke, and H. Berresheim (2004), Assessment of the applicability of $\text{NO}-\text{NO}_2-\text{O}_3$ photostationary state of long-term measurements at the Hohenpeissenberg GAW Station, Germany, *Atmos. Chem. Phys.*, *4*, 1265–1277.
- Martin, R. V., C. E. Sioris, K. Chance, T. B. Ryerson, T. H. Bertram, P. J. Wooldridge, R. C. Cohen, J. A. Neuman, A. Swanson, and F. M. Flocke (2006), Evaluation of space-based constraints on nitrogen oxide emissions with regional aircraft measurements over and downwind of eastern North America, *J. Geophys. Res.*, *111*, D15308, doi:10.1029/2005JD006680.
- Monks, P. S. (2000), A review of the observations and origins of the spring ozone maximum, *Atmos. Environ.*, *34*, 3545–3561.
- Munger, J. W., S. C. Wofsy, P. S. Bakwin, S.-M. Fan, M. L. Goulden, B. C. Daube, A. H. Goldstein, K. E. Moore, and D. R. Fitzjarrald (1996), Atmospheric deposition of reactive nitrogen oxides and ozone in a temperate forest and a subarctic woodland I. Measurements and mechanisms, *J. Geophys. Res.*, *101*, 12,639–12,657.
- Murphy, J. G., D. A. Day, P. A. Cleary, P. J. Wooldridge, and R. C. Cohen (2006), Observations of the diurnal and seasonal trends in nitrogen oxides in the western Sierra Nevada, *Atmos. Chem. Phys.*, *6*, 5321–5338.
- Nakamura, K., et al. (2003), Measurement of NO_2 by the photolysis conversion technique during the Transport and Chemical Evolution Over the Pacific (TRACE-P) campaign, *J. Geophys. Res.*, *108*(D24), 4752, doi:10.1029/2003JD003712.
- Nenes, A., S. N. Pandis, and C. Pilinis (1998), ISORROPIA: A new thermodynamic equilibrium model for multiphase multicomponent inorganic aerosols, *Aquat. Geochem.*, *4*, 123–152.
- Nenes, A., S. N. Pandis, and C. Pilinis (1999), Continued development and testing of a new thermodynamic aerosol module for urban and regional air quality models, *Atmos. Environ.*, *33*, 1553–1560.
- Neuman, J. A., L. G. Huey, T. B. Ryerson, and D. W. Fahey (1999), Study of inlet materials for sampling atmospheric nitric acid, *Environ. Sci. Technol.*, *33*, 1133–1136.
- Ordóñez, C., A. Richter, M. Steinbacher, C. Zellweger, H. Nüss, J. P. Burrows, and A. S. H. Prévôt (2006), Comparison between 7 years of satellite-borne and ground-based tropospheric NO_2 measurements around Milan, Italy, *J. Geophys. Res.*, *111*, D05310, doi:10.1029/2005JD006305.
- Osthoff, H. D., et al. (2006), Measurement of atmospheric NO_2 by pulsed cavity ring-down spectroscopy, *J. Geophys. Res.*, *111*, D12305, doi:10.1029/2005JD006942.
- Penner, J. E., C. S. Atherton, J. Dignon, S. J. Ghan, J. J. Walton, and S. Hameed (1991), Tropospheric nitrogen—A 3-dimensional study of sources, distributions, and deposition, *J. Geophys. Res.*, [Atmos.], *96*, 959–990.
- Platt, U., and D. Perner (1980), Direct measurements of atmospheric CH_2O , HNO_2 , NO_2 , and SO_2 by differential optical absorption in the near UV, *J. Geophys. Res.*, C: Oceans Atmos., *85*, 7453–7458.
- Richter, A., J. P. Burrows, H. Nüss, C. Granier, and U. Niemeier (2005), Increase in tropospheric nitrogen dioxide over China observed from space, *Nature*, *437*, 129–132.
- Roberts, J. M. (1995), Reactive odd-nitrogen (NO_y) in the atmosphere, in *Composition, Chemistry, and Climate of the Atmosphere*, edited by H. B. Singh, pp. 176–215, Van Nostrand Reinhold, Hoboken, N. J.
- Ryerson, T. B., E. J. Williams, and F. C. Fehsenfeld (2000), An efficient photolysis system for fast-response NO_2 measurements, *J. Geophys. Res.*, D21.
- Schaub, D., K. F. Boersma, J. W. Kaiser, A. K. Weiss, D. Folini, H. J. Eskes, and B. Buchmann (2006), Comparison of GOME tropospheric NO_2 columns with NO_2 profiles deduced from ground-based in situ measurements, *Atmos. Chem. Phys.*, *6*, 3211–3229.
- Staffelbach, T., et al. (1997), Photochemical oxidant formation over southern Switzerland. I. Results from summer 1994, *J. Geophys. Res.*, *102*, 23,345–23,362.
- Stedman, D. H., and M. J. McEwan (1983), Oxides of nitrogen at two sites in New Zealand, *Geophys. Res. Lett.*, *10*, 168–171.
- Steinbacher, M., S. Henne, J. Dommen, P. Wiesen, and A. S. H. Prévôt (2004), Nocturnal trans-alpine transport of ozone and its effects on air quality on the Swiss Plateau, *Atmos. Environ.*, *38*, 4539–4550.
- Stutz, J., B. Alicke, and A. Neftel (2002), Nitrous acid formation in the urban atmosphere: Gradient measurements of NO_2 and HONO over grass in Milan, Italy, *J. Geophys. Res.*, *107*(D22), 8192, doi:10.1029/2001JD000390.
- Swiss National Air Pollution Monitoring Network (NABEL) (2005), Technischer Bericht zum Nationalen Beobachtungsnetz für Luftfremdstoffe (NABEL), Empa Material Science & Technology, Duebendorf.
- Thomberry, T., et al. (2001), Observations of reactive oxidized nitrogen and speciation of NO_y during the PROPHET summer 1998 intensive, *J. Geophys. Res.*, *106*, 24,359–24,386.
- Thornton, J. A., P. J. Wooldridge, and R. C. Cohen (2000), Atmospheric NO_2 : in situ laser induced fluorescence detection at parts per trillion mixing ratios, *Anal. Chem.*, *72*, 528–539.
- Thornton, J. A., P. J. Wooldridge, R. C. Cohen, E. J. Williams, D. Hereid, F. C. Fehsenfeld, J. Stutz, and B. Alicke (2003), Comparisons of in situ and long path measurements of NO_2 in urban plumes, *J. Geophys. Res.*, *108*(D16), 4496, doi:10.1029/2003JD003559.
- Volz-Thomas, A., H. W. Pätz, N. Houben, S. Konrad, D. Mihelcic, T. Klüpfel, and D. Perner (2003), Inorganic trace gases and peroxy radicals during BERLIOZ at Pabstthum: An investigation of the photostationary state of NO_x and O_3 , *J. Geophys. Res.*, *108*(D4), 8248, doi:10.1029/2001JD001255.
- Volz-Thomas, A., M. Berg, T. Heil, N. Houben, A. Lerner, W. Petrick, D. Raak, and H. W. Pätz (2005), Measurements of total odd nitrogen (NO_y) aboard MOZAC in-service aircraft: Instrument design, operation, and performance, *Atmos. Chem. Phys.*, *5*, 583–595.

- Williams, E. J., et al. (1998), Intercomparison of ground based NO_y measurement techniques, *J. Geophys. Res.*, *103*, 22,261–22,280.
- Winer, A. M., J. W. Peters, J. P. Smith, and J. N. Pitts Jr. (1974), Response of commercial chemiluminescence $\text{NO}-\text{NO}_2$ analyzers to other nitrogen-containing compounds, *Environ. Sci. Technol.*, *8*, 1118–1121.
- Wunderli, S., and R. Gehrig (1991), Influence of temperature on formation and stability of surface PAN and ozone. A two year field study in Switzerland, *Atmos. Environ.*, *25A*, 1599–1608.
- Zanis, P., A. Ganser, C. Zellweger, S. Henne, M. Steinbacher, and J. Staehelin (2007), Seasonal variability of measured ozone production efficiencies in the lower free troposphere of Central Europe, *Atmos. Chem. Phys.*, *7*, 223–236.
- Zellweger, C., M. Ammann, P. Hofer, and U. Baltensperger (1999), NO_y specification with a combined wet effluent diffusion denuder-aerosol collector coupled to ion chromatography, *Atmos. Environ.*, *33*, 1131–1140.
- Zellweger, C., M. Ammann, B. Buchmann, P. Hofer, M. Lugauer, R. Rüttimann, N. Streit, E. Weingartner, and U. Baltensperger (2000), Summertime NO_y speciation at the Jungfrauoch, 3580 m above sea level, Switzerland, *J. Geophys. Res.*, *105*, 6655–6667.
- Zellweger, C., J. Forrer, P. Hofer, S. Nyeki, B. Schwarzenbach, E. Weingartner, M. Ammann, and U. Baltensperger (2003), Partitioning of reactive nitrogen (NO_y) and dependence on meteorological conditions in the lower free troposphere, *Atmos. Chem. Phys.*, *3*, 779–796.
-
- B. Buchmann, S. Bugmann, C. Hueglin, B. Schwarzenbach, M. Steinbacher, and C. Zellweger, Laboratory for Air Pollution/Environmental Technology, Empa, Swiss Federal Institute for Materials Science and Technology, Empa, CH-8600, Dübendorf, Switzerland. (martin.steinbacher@empa.ch)
- C. Ordóñez, Laboratoire d'Aérodologie, Toulouse, France.
- A. S. H. Prevot, Laboratory of Atmospheric Chemistry, Paul Scherrer Institute, Villigen PSI, Switzerland.